

Framework for Simulating Fracture, Ejection, and Restraint of Rock around a Mine Drift Subjected to Seismic Loading

Raffaldi, M.J.

National Institute for Occupational Safety and Health, Spokane, WA, USA

Loken, M.C.

M&K Consulting, Saint Paul, MN, USA

Copyright 2016 ARMA, American Rock Mechanics Association

This paper was prepared for presentation at the 50th US Rock Mechanics / Geomechanics Symposium held in Houston, Texas, USA, 26-29 June 2016. This paper was selected for presentation at the symposium by an ARMA Technical Program Committee based on a technical and critical review of the paper by a minimum of two technical reviewers. The material, as presented, does not necessarily reflect any position of ARMA, its officers, or members. Electronic reproduction, distribution, or storage of any part of this paper for commercial purposes without the written consent of ARMA is prohibited. Permission to reproduce in print is restricted to an abstract of not more than 200 words; illustrations may not be copied. The abstract must contain conspicuous acknowledgement of where and by whom the paper was presented.

ABSTRACT: Researchers at the National Institute for Occupational Safety and Health (NIOSH), Spokane Mining Research Division (SMRD) have developed a modeling framework, using commercially available software, for investigating the fracture and ejection of rock into underground mine openings caused by seismic loading and the restraint of this failed rock by the ground support system. The modeling framework presented here establishes the conceptual foundation and demonstrates the required capabilities for a model of a simple two-dimensional cross-section of a deep mine drift. The model has been used to investigate the effects of various wave parameters on the stability of underground excavations, both with and without ground support. Additionally, kinetic energy of ejected rock and energy dissipated by the ground support system are calculated and compared. Finally, the effectiveness of ground support, with and without containment, has been investigated. The main conclusion is that simplified empirical rockburst damage analyses based solely on volume of ejected rock are inadequate. The damage potential of a seismic event should be measured in terms of dynamic energy demand on the ground support. Further, peak specific power may be a better wave parameter to correlate with this demand. This research aids in the understanding of the effects of mining induced seismic loading on underground excavations and support systems, and may lead to improvements in miner safety.

1. INTRODUCTION

Continued advancement of computing technology and capabilities of commercially available numerical modeling software has made fully-dynamic numerical simulation of problems in geomechanics more practical than ever before. However, application of this technology is still not common place (as compared with static numerical modeling).

Numerical modeling in geomechanics is associated with unique and significant challenges because of the uncertainty involved with engineering of natural systems. In rock mechanics, this uncertainty stems primarily from inherent complexities associated with geologic materials. Often times, even for static or quasi-static problems, it is not feasible to incorporate these complexities into a model, resulting in solutions that have high margins of error; the problem is data-limited.

Solutions to dynamic problems in geomechanics are therefore hampered from the outset, because the dynamic solution is dependent upon the initial conditions, which are generally the static equilibrium state of the excavation, which is itself a data-limited

problem. Additionally, there is uncertainty surrounding nearly every aspect of the dynamic solution. For a mining rockburst this includes dynamic behavior of intact rock, discontinuities, and ground support; source mechanism; the characteristics of the ground motion and the changes that occur as the wave propagates through the rock mass (path effects); and interactions between the seismic waves, excavation, and ground support.

Rockbursting is one of the greatest challenges in mining ground control. Though not all rockbursts cause damage, and fortunately, even fewer result in injury or fatality to underground workers, the economic and human consequences of a rockburst can be severe. Research in recent decades has focused primarily on the dynamic testing of ground support components. However, in order to better understand the load demands placed on ground support, fully-dynamic numerical modeling will need to play a larger role in research.

The current state of understanding is such that mechanism identification and qualitative parameter study can play an important role. Simple models that capture mechanically significant features have often been valuable in data-limited fields such as

geomechanics (Starfield and Cundall, 1988). The process of modeling, in and of itself, forces us to break the problem down into a mechanical system, and the attempt to understand this system may sometimes be more important than the prediction itself (Barbour and Krahn, 2004). Incorporation of simple numerical modeling into mining rock mechanics facilitates (Hammah and Curran, 2009):

- (i) Development of understanding,
- (ii) Proper formulation of questions,
- (iii) Reasonable approximation of behavior and provision of meaningful predictions, and
- (iv) Aids in the design of solutions and decision making.

This paper presents a framework for fully-dynamic modeling of the fracture, ejection, and restraint of rock around a mine drift subject to seismic loading from a remote source. The model presented in this paper is used to (1) investigate the relationship between seismic wave parameters and rock mass damage, (2) quantify the kinetic energy (KE) of the ejected rock during a seismic event, (3) quantify the energy dissipated by plastic deformation of the ground support system, and (4) investigate how the ground support system acts to support an excavation during seismic loading. This paper is concerned with a remotely triggered event where damage occurs as rockfalls induced by seismic shaking and rock ejection caused by seismic energy transfer.

2. BACKGROUND

A rockburst can be defined as damage to an excavation that occurs in a sudden or violent manner and is associated with a seismic event (Kaiser et al., 1996). The key difference between a rockburst and a seismic event is that a rockburst involves damage to an excavation.

This leads to the classification of rockbursts as either self-initiated or remotely triggered (Kaiser et al., 1996). A self-initiated rockburst occurs when the seismic event and damage location coincide, while a remotely triggered rockburst occurs when a seismic wave, generated from a remote source, results in dynamic stresses sufficient to cause damage to an excavation some distance from the source. Examples of self-initiated bursts include strain bursts and pillar bursts. Remotely triggered events include damage caused by a seismic wave generated from a fault-slip or a remote burst event.

There are three fundamental categories of rockburst damage mechanisms (Kaiser et al., 1996): (1) rock bulking due to fracturing, (2) rock ejection due to seismic energy transfer, and (3) rockfalls induced by seismic shaking. The severity of rockburst damage can range from minor (surface spalls and shallow slabbing)

to major (damage of a meter or more into the excavation wall) (Kaiser et al., 1996).

One method of controlling rockburst damage is to limit the number and severity of events by altering mining methods and development plans. However, the seismic response of ground to mining cannot be entirely eliminated, so associated damage must be mitigated using dynamic ground support. The main concern is ensuring that the capacity of the ground support system can withstand the dynamic demands imposed on it. Some of the issues associated with understanding the demand on, and the capacity of, the support system are discussed here.

The two most important factors influencing the severity of a rockburst—and thus the demand on the ground support—are the magnitude of the event, and the proximity of the event to the excavation (Potvin and Wesseloo, 2013). However, there are many other factors that may play a role in the severity of damage including: rock strength, rock structure and condition, in situ and mining induced stress conditions, excavation geometry, ground support choice, and the source mechanism. For a remotely triggered rockburst, complexities associated with generation of a seismic wave, the radiation, reflection, and refraction of this wave as it travels through the rock mass, and its interaction with the excavation and ground support have resulted in the adoption of very simplistic methodologies to estimate the dynamic demand.

The intensity of a propagating seismic wave decreases with distance due to geometric spreading and attenuation. Therefore, knowledge of both the event magnitude and the distance from mine openings is required to estimate the demand on the ground support. In mining, the most common method used to characterize the dynamic demand has been to assume that it is a function of a single wave parameter, usually peak particle velocity (PPV). Peak particle acceleration (PPA) has sometimes been used in other branches of geotechnical engineering.

McGarr et al. (1981) showed that PPV correlates directly with peak transient stress making it the most appropriate parameter for damage assessment, but Dowding (1985) has suggested that whether acceleration, velocity, or displacement is the most appropriate to measure depends on the frequency content of the wave. McGarr (1983) listed several advantages to using PPV instead of PPA as a measure of ground motion resulting from mining induced seismicity, including: (1) for a given event magnitude, PPV falls within a much narrower range than PPA, (2) it also better correlates with structural damage (McGarr, 1981), and (3) time histories of ground velocity can more readily be synthesized as a function of seismic event size. McGarr (1983) also noted that the value of PPA

can often be very large, even when PPV is low, without damage occurring to excavations. Empirical scaling laws that express the PPV of a seismic wave as a function of event magnitude and distance to source are often used to estimate support demand (Hedley, 1992; Kaiser et al., 1996).

In other branches of geotechnical engineering it has been common to determine damage thresholds based on PPV and/or PPA. Examples of this approach include the work of Dowding and Rosen (1978), Sharma and Judd (1991), Langefors and Kihlstrom (1963), Bauer and Calder (1970), and Hendron (1977). In the rockbursting mines of the Witwatersrand region of South Africa it has been observed that generally, when PPV of a mining induced seismic event remains below about 1 m/s, little damage occurs (Wagner 1984). However, Cichowicz et al. (2000) reported that an analysis of rockburst damage at East Rand Proprietary Mine showed that significant damage sometimes occurred even when estimated PPV was lower than 1 m/s.

While PPV has been observed to scale well with event magnitude and distance from the source, attempts to relate rockburst damage with PPV have often resulted in poor correlation (Potvin and Wesseloo, 2013). A recent analysis of rockburst data from the Creighton Mine in Ontario Canada (Morissette et al., 2012) concluded that the amount of displaced rock had no apparent correlation with PPV as predicted by empirical scaling laws. While PPV may be an acceptable indicator of the intensity of a seismic wave, seismic loading and damage appears to be more complex than to be summarized by a single seismic parameter.

The work of Barton and Hansteen (1979), Brady (1990), Hsiung et al. (1992), Ma and Brady (1999), and Hsiung and Ghosh (2006) demonstrated that simple PPV or PPA damage thresholds were not fully adequate to evaluate the stability of excavations in jointed rock. Through field measurements, scale and numerical modeling, these studies demonstrated that cumulative movements occur along joints during successive seismic events.

St. John and Zarrah (1987) have advocated that duration and energy content of the seismic loading are also key to determining damage. Labreche (1983), via field testing, concluded that the extent of damage in underground rock tunnels subjected to blast vibrations was frequency dependent. Dowding et al. (1983) constructed a model of an underground cavern subjected to earthquake loading and found that the magnitude of closure, which occurred due to frictional sliding along joints, was also dependent on frequency.

Frequency may also be an important factor when considering the *site effect* (Cichowicz et al., 2000). The *site effect* is a term that refers to amplification of a seismic wave due to the excavation geometry, the

presence of a free surface, and the surrounding zone of fractured rock. It has been observed that PPV at an excavation surface can be amplified by as much as 10 times that of the constrained wave (Milev et al., 1999; Durrheim et al., 1998; Cichowicz, 2000). The amplification of waves in the vicinity of an excavation has been observed to be highly variable, even within the same mine (Webber, 2000). Potvin and Wesseloo (2013) provide a more in depth review of the complexities associated with determining the dynamic demand on ground support.

A complete ground support system is composed of three main components (Ortlepp, 1983; Potvin et al., 2010): reinforcement (bolts and cables), containment (surface support), and connections. The reinforcing components act to maintain integrity of the fractured rock surrounding the excavation. The surface support helps maintain stability of the rock mass between the bolts by preventing unraveling and ejection. The connections allow load transfer to occur from the surface support to the reinforcement. Although bolts and cables are the critical components that stabilize the rockmass surrounding an excavation, any dynamic ground support system is only as effective as its weakest link (Potvin et al., 2010).

For a remotely triggered rockburst where the major damage mechanism is rockfalls caused by seismic shaking, the ground support is required to reinforce the rock mass by holding rock blocks and fragments in place and maintaining a support arch (Kaiser et al., 1996). When the damage mechanism is dynamic ejection of rock, the ground support elements will be required to maintain their integrity while yielding through large displacements, under high strain rates, to dissipate the KE of ejecting rock, thus bringing the ejected rock to rest (Wagner, 1984; Kaiser et al., 1996). Kaiser et al. (1996) reported that, generally, in rockburst-prone mines, ejection velocities below 1.5 m/s can be handled by standard ground support, but additional support is required for higher velocities; if average ejection velocity exceeds 5 m/s, ground support will generally not be effective.

In recent years, the vast majority of rockburst related research has focused on evaluation of the capacity of ground support via laboratory mechanical tests and field-scale blast tests. Laboratory testing of ground support has primarily focused on determining the dynamic capacity of individual support components via drop-type tests (Stacey, 2012). Though work of this type is important for understanding the relative performance of both reinforcement and support when subjected to dynamic loading, the applied loads are significantly different than that of real rockburst loading (Stacey, 2012). Momentum transfer type tests (Player et al., 2009; Thompson et al., 2009) are a significant

improvement but are still simplistic when compared to real rockburst loading, and like most lab tests, focus only on single components rather than the complete support system. Underground blast testing has the advantage that the complete support system can be evaluated as installed, but these tests are also limited in that they are expensive, the loading is still quite different from that of a rockburst, and the test conditions are rarely repeatable (Stacey, 2012). Hadjigeorgiou and Potvin (2007) and Stacey (2012) provide excellent reviews on the testing of ground support for rockburst conditions.

3. DYNAMIC MODELING CONSIDERATIONS

The process of developing a fully-dynamic numerical model and performing simulations is similar to that of a static model. The first step in the process is to establish initial conditions for the model. In geomechanics, this is usually the static equilibrium conditions of the system of interest. The dynamic loading simply adds several additional considerations and another layer of complexity to the modeling process. The basic steps required to develop a static numerical model are:

- (i) Develop model geometry
- (ii) Discretize the model
- (iii) Assign constitutive models and material properties
- (iv) Apply appropriate boundary and initial conditions
- (v) Establish initial equilibrium in the model
- (vi) Perform an alteration to the model
- (vii) Solve for the solution
- (viii) Evaluate the results and revise model if necessary

To expand the model to incorporate dynamic loading requires four additional considerations. These are:

- (ix) Wave transmission
- (x) Mechanical damping
- (xi) Dynamic boundary conditions
- (xii) Dynamic loading

Details on each of these steps and the basics of developing and running a dynamic model are provided by Raffaldi and Loken (2016).

4. MODEL DEVELOPMENT

The main purpose of the model was to develop a general framework for performing dynamic simulations in which rock fracture and ejection occurs as a result of dynamic loading from a remote mining induced seismic event. Additionally, the model was to be used to perform a preliminary investigation into the effects of seismic wave parameters on the dynamic stability of a generic metal mine drift. No site specific calibration was performed and the modeling approach focused on the investigation of mechanisms rather than site specific design, a methodology commonly required in geomechanics (Starfield and Cundall, 1988; Barbour and

Krahn, 2004; Hammah and Curran, 2009). The work presented in this paper operates on the left-hand side of Figure 1.

The numerical code UDEC (Universal Distinct Element Code) (Itasca, 2015) was chosen for this work. This program is based on the distinct element method and is applicable when a continuum analysis proves insufficient for a particular problem. In UDEC, the rock mass is represented as an assemblage of discrete blocks. Each discrete block may be discretized with a finite difference grid and subdivided into elements that individually deform in response to the applied forces or boundary constraints according to a prescribed stress-strain law. UDEC allows finite displacement and rotations between discrete blocks, including complete detachment, and it is capable of recognizing new contact surfaces automatically during the simulation.

Typical Situation	Complicated geology, inaccessible; no testing budget	←.....→	Simple geology, \$\$\$ spent on site investigation
Data	NONE	←.....→	COMPLETE
Approach	Investigation of Mechanisms	←.....→	Bracket field behavior by parameter studies Predictive (direct use in design)

Figure 1: Spectrum of Modeling Situations (Itasca, 2015)

The total number of input parameters required to solve this dynamic problem is in excess of fifty. These parameters can be classified into seven types, namely; (1) excavation geometry, (2) rock mass properties, (3) rock joint properties, (4) in situ stress conditions, (5) seismic source parameters, (6) rockbolt properties, and (7) liner properties.

4.1. Model Geometry

For simplicity, a plane-strain assumption was made. This makes it necessary to model only a slice through the tunnel cross section, because the out-of-plane direction is assumed to be infinite in length. An arched-roof was chosen for the drift cross-section, and the dimensions of the excavation cross-section are provided in Table 1.

Table 1. Drift Cross-Sectional Geometry

Parameter	Value	Units
Shape	Arched	-
Width	4.0	m
Spring Line Height	4.0	m
Total Height	4.8	m

4.2. Rock Mass Model and Properties

A rock mass model was developed in UDEC with the ability to:

- (i) Fail and deform in a ductile manner under high confinement,
- (ii) Fail in a brittle manner under low confinement,
- (iii) Fracture and allow discrete rock blocks to detach from the rockmass under both static and dynamic loads, and
- (iv) Transmit elastic waves without distortion.

The model is composed of three different parts: (1) the joints, (2) the joint model, and (3) the constitutive model. These three parts interact to determine the overall rock mass response. In this application, the purpose of the joints is to allow discrete rock blocks to fracture and eject, not to represent actual discontinuities in the rock. The joint model governs the behavior of these joints, while the constitutive model governs the behavior of the intact rock between the joints. The model is described in detail by Raffaldi and Loken (2016). Figure 2 below presents a conceptual diagram of the three parts of the model.

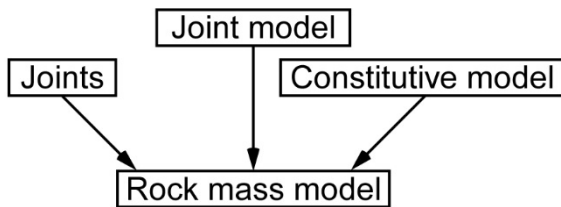


Figure 2: Conceptual diagram of rockmass model

A Mohr-Coulomb softening-hardening constitutive model was chosen to allow the material to behave in a ductile manner under high confining stresses. The tensile strength of the constitutive model was set to a large value to force tensile failure to occur through the joints. The constitutive model properties are presented in Table 2.

Table 2. Rock Mass Properties

Parameter	Value	Units
Density	2700.0	kg/m ³
Bulk Modulus	29.2	GPa
Shear Modulus	13.5	GPa
Peak Cohesion	16.0	MPa
Residual Cohesion	1.6	MPa
Peak Friction Angle	32.0	Deg.
Residual Friction Angle	32.0	Deg.
Peak Tensile Strength	∞	MPa
Residual Tensile Strength	∞	MPa

A Mohr-Coulomb model with residual strength was used for the joints. The joint stiffness values were assigned

large values such that they played a minimal role in the behavior of confined and/or non-fractured rock. Additionally, the joints were assigned a finite tensile strength to allow for failure and complete detachment of rock blocks depending on the loading conditions. The joint properties are shown in Table 3.

As previously stated, the purpose of the joint system is not to represent actual rock structure, but to allow a pathway for the rock to fracture. A randomized joint pattern was created using the Voronoi tessellation joint-generator embedded within UDEC. The joints separate the model into a system of distinct blocks. The Voronoi joint-generator requires several statistical inputs that control the average size and distribution of the blocks. The geometry of the block model around the excavation is shown below in Figure 3.

Table 3. Rock Joint Properties

Parameter	Value	Units
Normal Stiffness	292.0	GPa/m
Shear Stiffness	135.0	GPa/m
Peak Cohesion	16.0	MPa
Residual Cohesion	16.0	MPa
Peak Friction Angle	32.0	Deg.
Residual Friction Angle	32.0	Deg.
Peak Tensile Strength	0.5	MPa
Residual Tensile Strength	0	MPa

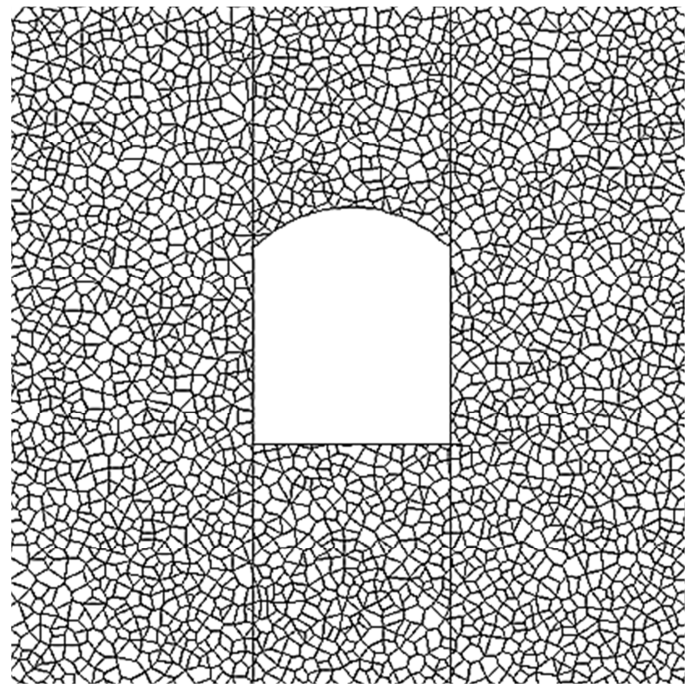


Figure 3: Example of Voronoi Block Model

UDec defaults were used for most of the Voronoi tessellation properties. The properties that were specified in the model are shown in Table 4. The Voronoi seed

value controls the starting point for the Voronoi tessellation. Changing the seed value will result in a similar but unique set of randomized joints. Other parameters, left with default settings, control properties such as block size uniformity.

4.3. Static Loading

For most of the modeling presented in this paper, an isotropic stress field of 50 MPa was used, except when the effects of in situ stress were investigated. The reason for doing so was to create a simple baseline case for use in parameter study. This value is the vertical stress magnitude associated with roughly 1850 m. of cover, assuming a vertical stress gradient of 0.027 MPa/m. This stress state was initialized in the model prior to excavation. Once the drift was excavated, the model was again brought to static equilibrium.

Table 4: Block and Voronoi Tessellation Properties

Property	Value	Units
Block Minimum Edge Length	0.025	m
Block Rounding Length	0.010	m
Overlap Tolerance	0.050	m
Voronoi Joint Average Edge Length	0.250	m
Voronoi Joint Seed Value	Variable	-

Table 5. In Situ Stress Parameters

Parameter	Value	Units
Vertical Stress (Depth)	50	MPa
Horizontal Stress Ratio	1	-

4.4. Seismic Source

The seismic source was specified as a shear wave input along an internal boundary designed to loosely represent the wave generated from a remote fault-slip source mechanism. In the modeling presented here, the source is located 25 meters from the excavation and has a length of 50 m. These dimensions are such that the entire excavation is enveloped by the wave. In this sense, the loading is similar to applying the wave along an external model boundary. However, the internal source allows for the wave to be applied at different angles to the excavation (although not done in this work) and forms a starting point for more accurate fault-slip source mechanism modeling in the future. The baseline case seismic source parameters are provided in Table 6. These parameters were used in all modeling cases unless otherwise specified.

Table 6. Seismic Source Parameters

Parameter	Value	Units
-----------	-------	-------

Frequency	40	Hz
PPV	2	m/s
Duration	0.25	sec
Distance	25	m
Orientation from horizontal	0	Deg.
Length	50	m

4.5. Dynamic Loading

One issue that arises when modeling strong ground motion, is how to specify the ground motion input. There are two options: (1) a synthetic waveform can be developed that represents the actual ground motion, or if ground motion records are available from the site of interest, (2) real waveforms may be used. Synthetic waveforms are used in this work, although the model can incorporate real measured seismic motion.

Ground vibrations incorporate many different frequency components but are often composed of a few dominant frequency bands. These dominant components can be determined from a Fourier transform of the wave. In this analysis the input waves are simplified to contain only a single frequency. This allows parameter studies to be performed to test the effect of a single frequency. It also prevents unneeded complexity from confusing the results. To specify transient loading, a bi-harmonic equation was used, defined by:

$$v(t) = (2)PPV[1 - \cos(2\pi f_1 t)][\sin(2\pi f_2 t)] \quad (1)$$

where,

$v(t)$ = velocity as a function of time

PPV = peak particle velocity

t = time

f_1 = major frequency

f_2 = minor frequency

Figure 4 graphically demonstrates the form of this wave function. The major frequency determines the duration of the dynamic loading. The minor frequency defines the frequency of the wave.

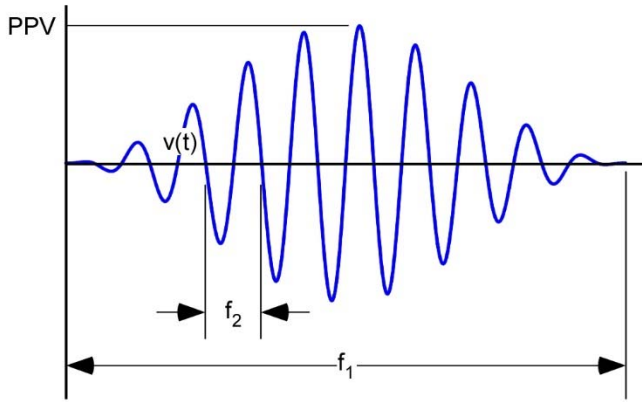


Figure 4. Synthetic Waveform Showing Peak Particle Velocity, Frequency, and Event Duration.

In addition to simplicity, conceptualizing the dynamic wave as a simple mathematical function prevents the need for applying a baseline correction and low-pass frequency filter to the input signal as would be required if real waveforms measured with a geophone or seismograph were used. This is because there is no error in the waveform due to instrument triggering and no high frequencies (short wavelengths) that cannot be modeled. During simulation, a quarter second quiet period was simulated after wave generation to allow time for the intact rock to again reach static equilibrium.

4.6. Dynamic Boundary Conditions

UDEC uses a quiet boundary scheme developed by Lysmer and Kuhlemeyer (1969). This type of dynamic boundary condition uses a series of dashpots that provide viscous normal and shear tractions that cancel out the dynamic stresses at the boundaries preventing them from being reflected back into the model. Quiet boundaries were used along the top, bottom, and sides of the model. These boundaries dissipate outgoing waves to prevent them from being reflected back toward the excavation.

4.7. Mechanical Damping

After performing several model runs, it was determined that it was not necessary to simulate material damping. For the modeled frequencies, only a few wavelengths can fit within the model boundaries. As a result, amplitude decay due to mechanical damping was insignificant compared to that caused by geometric spreading. Additionally, no abnormal oscillations were observed within the model when damping was not used. Finally, the incorporation of material damping into the models resulted in roughly an order of magnitude increase in run time. For these reasons, mechanical damping was neglected in each of the model runs presented in this paper. A schematic of the full model is shown in Figure 5.

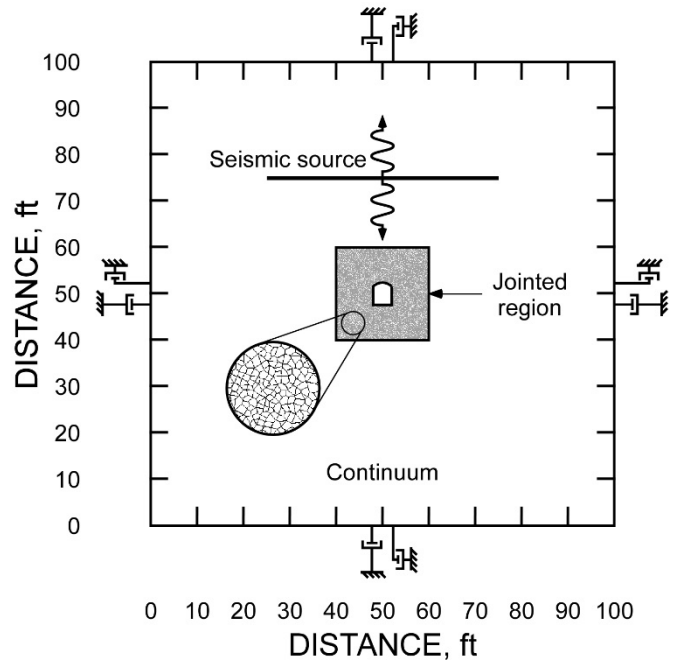


Figure 5: Schematic of Dynamic Distinct Element Model

5. IN SITU STRESS CONDITIONS

The chosen dynamic loading is characterized by a PPV of 2.0 m/s, frequency of 40 Hz, and a duration of 0.25 sec (plus a 0.25 sec quiet period). This model was used to perform a partial sensitivity analysis of the effect of in situ stress conditions on the resulting seismic damage for an unsupported excavation. First, five cases of increasing in situ stress magnitude were simulated, maintaining a vertical-to-horizontal stress ratio of 1.0. As shown in Figure 6, an increase in mass (volume) of displaced rock occurs with increasing in situ stress magnitude.

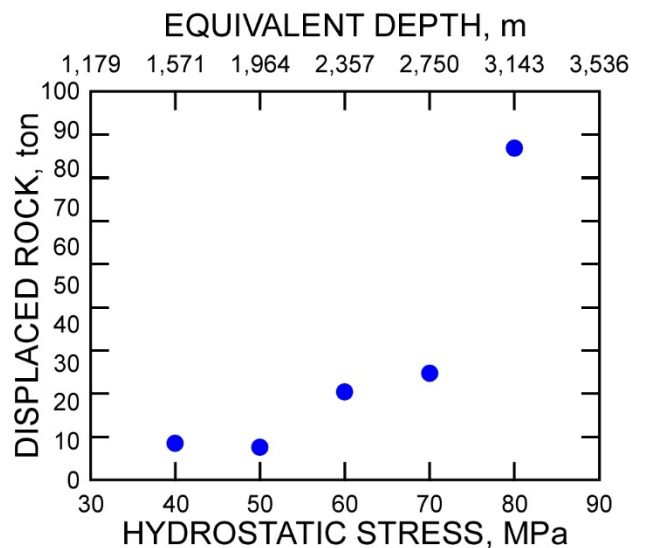


Figure 6: Displaced rock vs. stress for unsupported excavation subjected to 40 Hz wave with a PPV of 2.0 m/s and duration of 0.25 sec.

Six additional models were run introducing a deviatoric component to the in situ stress. A vertical stress (S_V) of 50 MPa was applied, but the horizontal stress (S_H) varied from 0.33 to 2.0 times the vertical. The results in Figure 7 show that S_V/S_H ratios that tend toward 1.0 result in less damage.

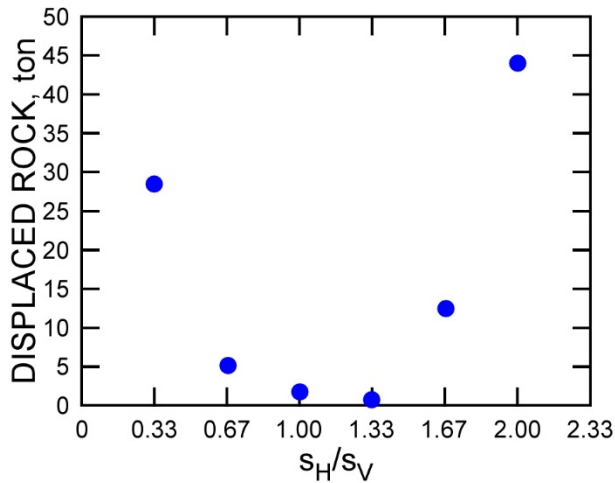


Figure 7: Displaced rock vs. horizontal-to-vertical stress ratio for unsupported excavation subjected to 40 Hz wave with a PPV of 2.0 m/s and duration of 0.25 sec.

Interestingly, in this simple model, differential in situ stress conditions have a greater effect than a hydrostatic stress increase equivalent to a depth increase of over 1,000 m. However, it should be noted that although the volume of damage is similar, the shape of the damaged excavation tends to form an ellipse with the long axis oriented perpendicular to the direction of major principal stress.

6. SEISMIC WAVE PARAMETER STUDY

Another parameter study was performed in order to investigate the effects of various wave parameters on seismic stability of the excavation. The model was initially subjected to waves with identical duration (0.25 sec) but different PPV and frequency. By keeping the duration constant for all the input waves, the radiated seismic energy (Perret, 1972) was kept constant for waves of equal PPV no matter the frequency. Radiated seismic energy is a measure of seismic source strength often used by seismologists and is the total energy associated with the motion propagated into a seismic region (Perret, 1972). It is proportional to the integral of the square of the velocity wave.

6.1. Peak Particle Velocity

The final states of the excavation after a full half second simulation (0.25 sec of loading, 0.25 sec quiet period) for 15 combinations of PPV and frequency, are shown in Figure 8. PPV was varied from 1 to 3 m/s in 0.5 m/s increments at frequencies of 20, 40 and 60 Hz.

At the final states shown in Figure 8, although the ejected rock has not reached static equilibrium, the wave has passed, and the volume of ejecting rock is no longer increasing. As expected, greater PPV results in more damage to the excavation. Additionally, the damage that occurs is also dependent on the frequency of the applied seismic wave. The ratio of displaced rock to excavation volume vs. PPV is shown in Figure 9. It is observed that the steepness of the curve is dependent upon the frequency of the applied wave. It is also observed that, for the frequencies considered, very little damage occurs until the PPV exceeds 1.5 m/s.

PPV is an important parameter because rock may be broken in tension by a reflected p-wave if the velocity amplitude is large enough. Additionally, the possible maximum ejection velocity of rock is often assumed to depend on the PPV of the seismic wave (Kaiser et al., 1996). Raffaldi and Loken (2016) simulated dynamic ejection of a block from a 1-D wave propagation model and found that the maximum ejection velocity that could be achieved was directly related to the PPV of the propagating wave (although the actual ejection velocity depended on multiple factors). The velocity of ejection is a critical variable with respect to determination of seismic support capacity, because the KE of the ejected rock (which is a function of mass and velocity) must be dissipated by the ground support system in order to bring the moving rockmass to rest.

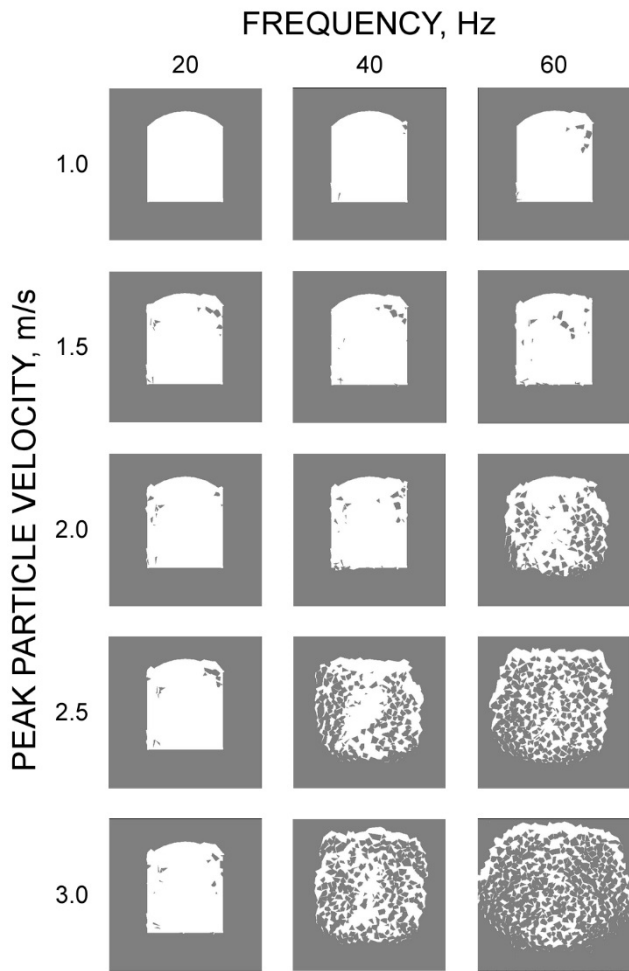


Figure 8: Final model states for unsupported excavation subjected to seismic waves of equal duration but varied PPV and frequency.

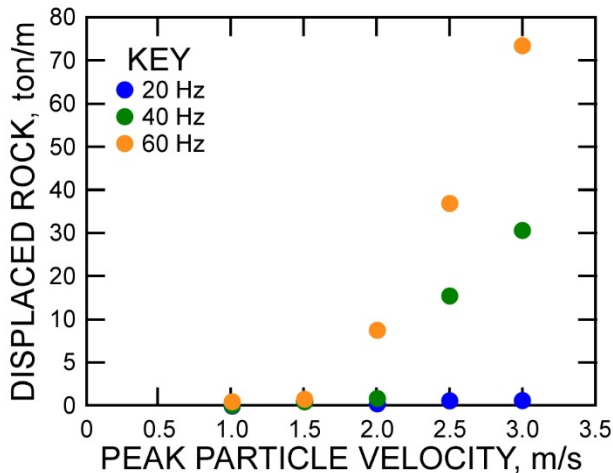


Figure 9: Weight of displaced rock vs. PPV for unsupported excavation subjected to seismic waves of equal duration.

Though not the focus of this paper, it is noteworthy that individual block ejection velocities, well in excess of twice the PPV of the applied seismic wave, were observed in the model. It should be noted that in the (1-D) modeling performed by Raffaldi and Loken (2016) ejection velocities greater than twice the PPV were not

obtained. The reason for the greater velocities was not determined, but such high velocities are consistent with field observations. Momentum exchange due to collisions between blocks of different masses seems a likely mechanism, but no conclusion can be drawn at this time. In the future, a carefully designed dynamic model might aid in understanding the site effect commonly observed in rockbursting mines.

6.2. Peak Particle Acceleration

Raffaldi and Loken (2016) suggested that ejection of rock in the vicinity of a free surface is better explained by acceleration than velocity. Although velocity directly corresponds to the state of stress in a constrained solid, acceleration is responsible for the damage near a free surface. For this reason, it was felt that PPA might better correspond with the modeled damage.

The accelerations associated with the velocity waves are readily calculated via differentiation. If the weight of displaced rock is instead plotted vs. PPA, as shown in Figure 10, an ostensible merging of the three frequency curves is noted. The remaining variation between the 40 and 60 Hz cases suggests a secondary influence. Most importantly, these results indicate that there is a particle acceleration threshold below which no damage will occur. Above this threshold, the level of damage will largely depend on the magnitude of the accelerations.

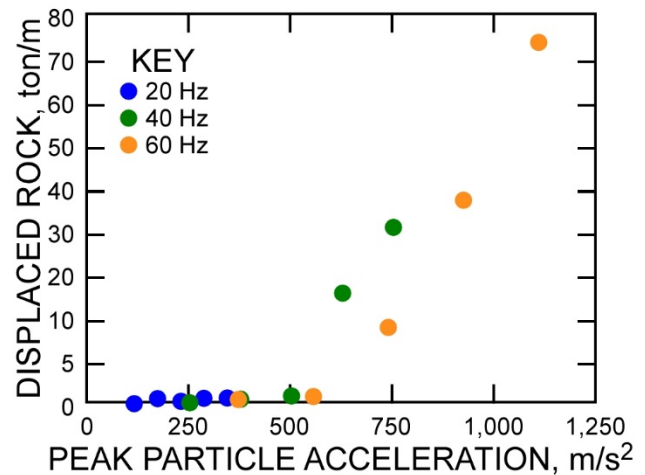


Figure 10: Weight of displaced rock vs. PPA for unsupported excavation subjected to seismic waves of equal duration.

6.3. Duration and Wave Cycles

In the previous section, as a result of maintaining constant radiated seismic energy between waves of the same PPV, the number of cycles in the wave was greater for higher frequency events. This potentially explains the results of Section 6.2. To determine the effect that this had on the modeled damage, an additional set of 15 modeling runs was simulated where the number of cycles was held constant. This required that lower frequencies have longer durations and therefore larger radiated seismic energy. A

0.25 sec quiet period was still included after the wave. The input waves are shown in Figure 11. Final state profiles are provided in Figure 12. Figures 13 and 14 show the displaced rock vs. PPV and PPA, respectively.

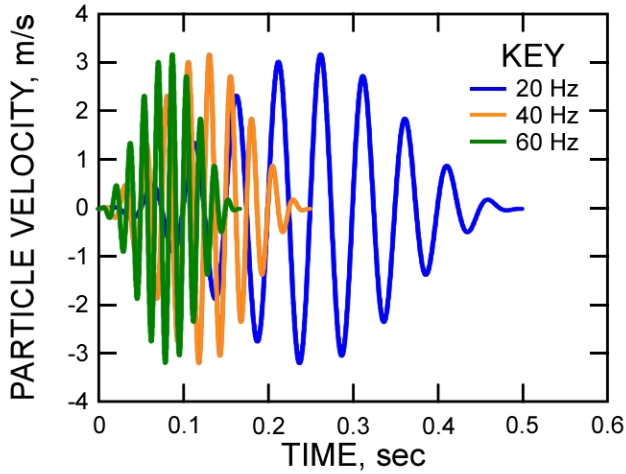


Figure 11. Example synthetic waveforms, with equal number of cycles, used for model input.

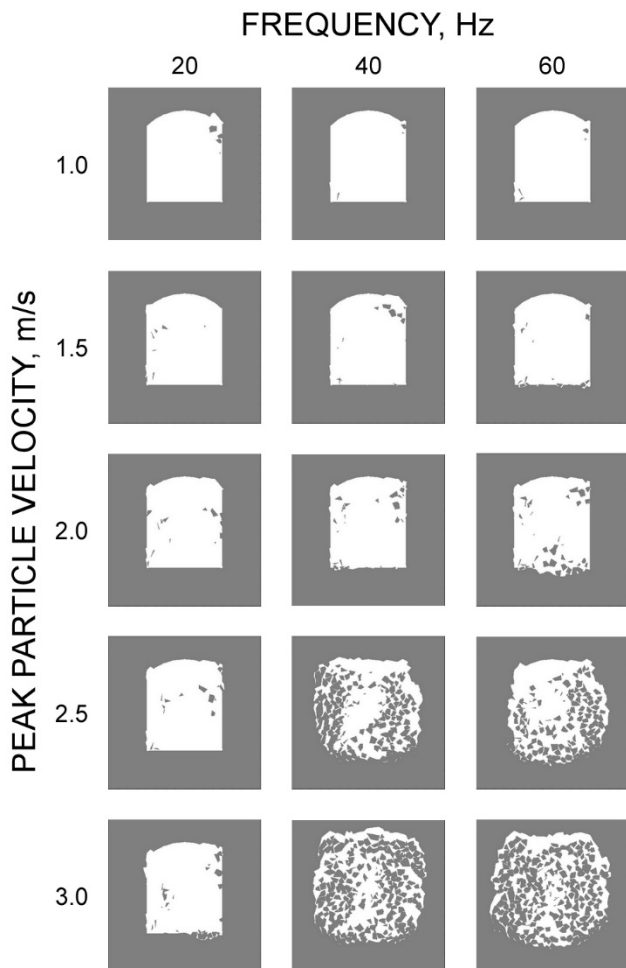


Figure 12: Final model states for unsupported excavation subjected to seismic waves of equal number of cycles.

It is observed in Figure 12 that for the 40 and 60 Hz waves, volume of ejected rock is well explained by PPV,

but that the relationship fails for the 20 Hz cases. Figure 14 shows that for waveforms of equal cycle count, the onset of ejection is still well explained by a PPA threshold, but that once this threshold is exceeded, PPA does not adequately explain the volume of rock that is ejected.

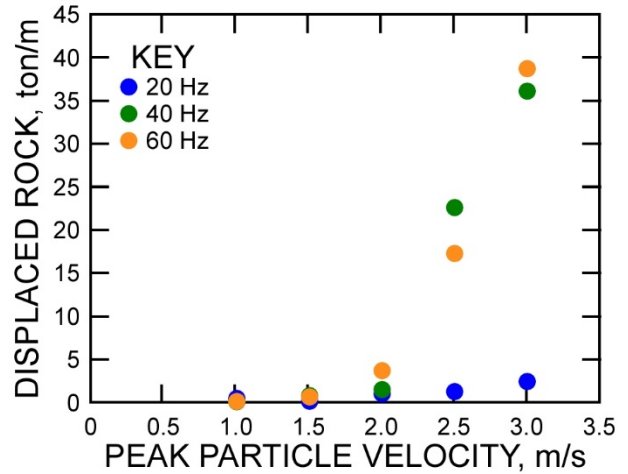


Figure 13: Weight of displaced rock vs. PPV for unsupported excavation subjected to seismic waves of equal number of cycles.

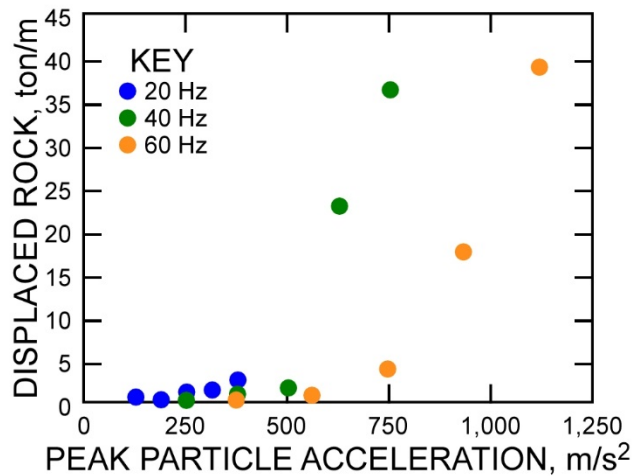


Figure 14: Weight of displaced rock vs. PPA for unsupported excavation subjected to seismic waves of equal number of cycles.

Raffaldi and Loken (2016) demonstrated only that 1-D ejection of a block (of fixed size) from a free surface was directly proportional to the acceleration of the block. PPA is only a measure of the peak acceleration contained in the waveform, and like PPV, does not appear to fully characterize the dynamic loading.

Raffaldi and Loken (2016) also show that for a given joint strength and PPV, the ejection velocity of a block at the surface of a 1-D rod will increase with increasing wave frequency. It is likely that defining damage solely as the mass of ejected rock may not be adequate, and that both mass and velocity should be considered. Therefore, to adequately assess the severity of the

seismic loading, the KE of the displaced rock (the maximum dynamic energy demand) should be calculated.

7. ENERGY CALCULATIONS

During seismic loading of an underground excavation in rock, it is logical to assume that, as a result of the principle of conservation of energy, part of the energy associated with the wave will transfer through the rock surrounding the excavation, part will be reflected back at the free surfaces of the excavation, part will be dissipated via rock fracture and frictional sliding, and part will be transferred to ejected rock fragments as KE. The distribution of the energy will depend upon the strength of the intact rock and discontinuities, as well as the characteristics of the seismic wave. The dynamic energy demand on the ground support system depends on the mass and velocity of this ejecting rock, regardless of the original energy of the seismic wave. If no rock ejects from an unsupported excavation, then the rock mass is capable of supporting itself, and there is no need for a support system. However, if large volumes of rock eject at high velocity, ground support with a high energy capacity will be required to control this ejection.

NIOSH contracted with Itasca to develop new energy calculation features within UDEC 6.0 (Christianson, 2015). These features calculate and report KE of ejecting rock and energy dissipated by the ground support system at each time step. Groups of blocks and clusters of blocks that have broken away from the main rock mass are detected by assuming that any block (or cluster of blocks) that has fractured all the way around its perimeter is loose. The KE of loose blocks is considered to be the KE of ejected rock. The structural support energy dissipation calculation includes energy dissipation during axial yielding, node slip (representing slip along the bolt-grout or liner-rock interfaces), and plastic bending of both rockbolt and liner structural elements (SELS). These new features allow the KE associated with the ejecting rock, and the energy dissipated by the ground support system, to be calculated and compared between different cases.

8. GROUND SUPPORT MODELING

The same models from Section 6.3 were reanalyzed after the installation of simple ground support. The ground support consisted of perfectly plastic rockbolt and liner SELs. The SELs were intended to represent generic yielding rockbolts and generic yielding surface support. The properties are listed for the rockbolts in Tables 7 and 8, and for the liner in Tables 9 and 10. It was decided not to allow the ground support to rupture. In this way, the total energy demand on the ground support could be evaluated.

In UDEC, rockbolts are modeled using a series of two-dimensional (2-D) elements with three degrees of freedom at each node (two translational and one rotational). The rockbolt elements can deform axially in response to applied loads. The distributed mass of the rockbolt is lumped at the structural element nodes which move in response to applied forces and moments according to the equations of motion. Material behavior is elastic perfectly-plastic. Additionally, the rockbolts are coupled at their nodes to the UDEC model via shear and normal springs that transfer forces and motion between the rockbolt elements and the grid points of the zones in which the rockbolt nodes reside. The normal and shear spring strength is defined via normal and shear cohesion and friction angles. The rockbolt model also allows for yield in bending at the nodes.

Table 7. Rockbolt Properties

Parameter	Value	Units
Young's Modulus	200.0	GPa
Yield Stress	500.0	MPa
Rupture Strain	∞	%
Density	7800.0	kg/m ³
Diameter	0.011	m
Length	2.0	m
Spacing	1.0	m
Pretension Force	30.0	kN

Table 8. Rockbolt Grout Properties

Parameter	Value	Units
Cohesion	10.0	MN/m/m
Friction Angle	10.0	deg.
Hole Diameter	0.034	m
Shear Stiffness	10.0	MN/m/m

Table 9. Reinforced Shotcrete Liner Properties

Parameter	Value	Units
Young's Modulus	20.0	GPa
Poisson's Ratio	0.15	---
Compressive Strength	35.0	MPa
Peak Tensile Strength	4.0	MPa
Residual Tensile Strength	3.0	MPa
Density	2300.0	kg/m ³
Thickness	0.07	m

Surface support consists of a series of beam elements that deform in response to applied axial, transverse, and flexural loads. Mass is lumped at grid points. The bond between the liner and rock surface occurs via radial and tangential connecting springs. Beam elements are elastic-perfectly plastic.

Table 10. Reinforced Shotcrete Interface Properties

Parameter	Value	Units
Cohesion	0.5	MPa
Tensile Strength	0.5	MPa
Friction Angle	35.0	deg.
Normal Stiffness	1.0	GPa/m
Shear Stiffness	1.0	GPa/m

8.1. Rockbolt Reinforcement

Installation of yielding rockbolts severely limited the volume of rock that ejected into the excavation. This is observed by comparing Figure 15 to Figure 12.

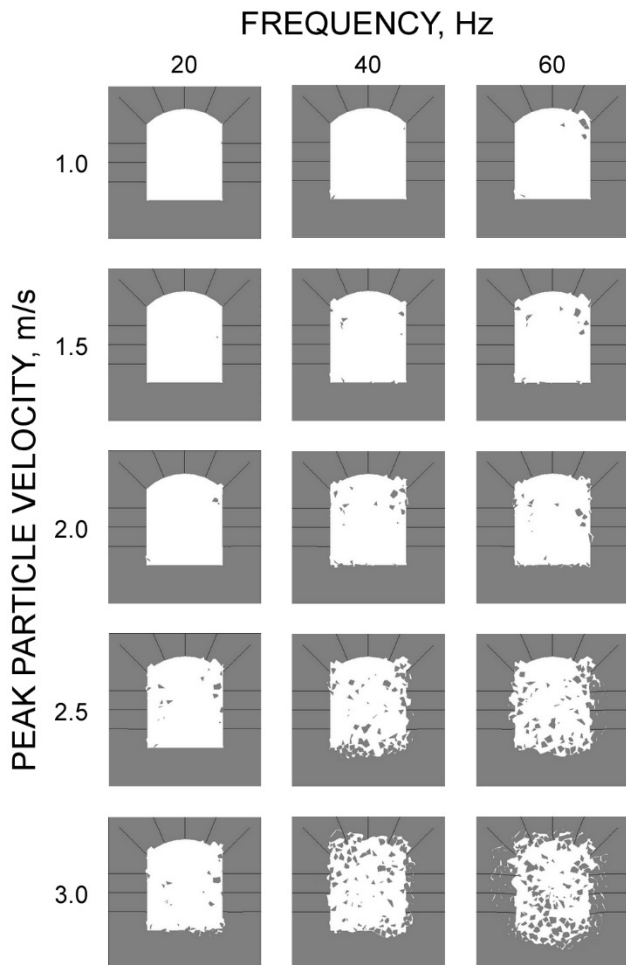


Figure 15: Final model states for rockbolt reinforced excavation subjected to seismic waves of equal number of cycles.

However, as might be expected, loose blocks between the bolts ejected into the excavation. The rock ejected between bolts represents rock that would contribute to the load demand on the surface support. An interesting observation is that although the 40 and 60 Hz waves (of equal cycle count) resulted in similar ejected volumes of rock for similar particle velocities, the dynamic demand on the ground support was clearly greater for the 60 Hz waves. This is observed indirectly by looking at the damage to the rock surrounding the excavation, and directly by calculating the energy dissipated by the ground support through plastic deformation and bolt pull out. Figures 16 and 17 show the joint fracturing that occurred around the reinforced excavation for the 2.5 and 3.0 m/s PPV waves with 40 and 60 Hz frequencies. It is observed that even though the mass of ejected rock for unsupported cases is similar, the extent of fracturing is greater when a 60 Hz wave is used. In section 9.0, it is shown that energy dissipated by ground support for 60 Hz cases is much greater as well.

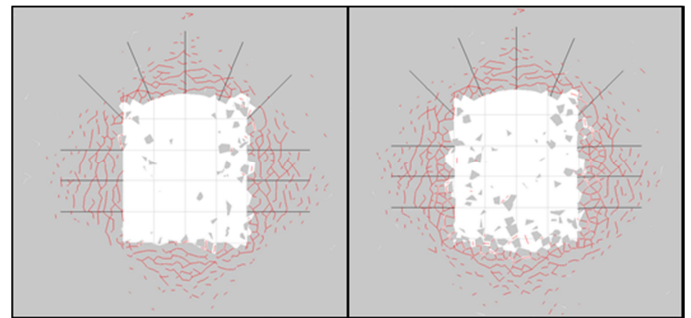


Figure 16: Comparison of rock fracturing for 2.5 m/s waves of equal number of cycles for (left) 40 Hz wave and (right) 60 Hz wave.

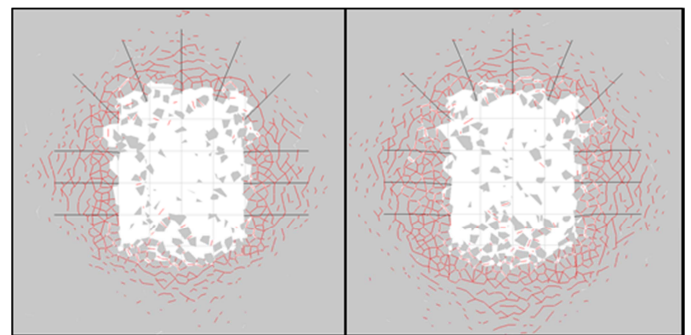


Figure 17: Comparison of rock fracturing for 3.0 m/s waves of equal number of cycles for (left) 40 Hz wave and (right) 60 Hz wave.

8.2. Surface Support

Dynamic models that included both reinforcement and surface support took a considerable amount of time to run to completion (days) and were therefore not fully included in this paper. However, a single model was run to completion using the seismic loading case of 3.0 m/s PPV and 60 Hz frequency. The final state profile of the tunnel for (a) unsupported, (b) bolted, and (c) bolted and lined cases is shown in figure 18. It should be mentioned

that in case (c), the liner is connected to the bolts to form a complete ground support system. As is common in practice, the floor of the excavation is not supported.

It is seen that the bolts are the primary element of the ground support system, but that a well-connected liner is required for retainment of rock ejecting between the bolts. The KE of the ejecting rock vs. time, for each of the three cases, is plotted in Figure 19.

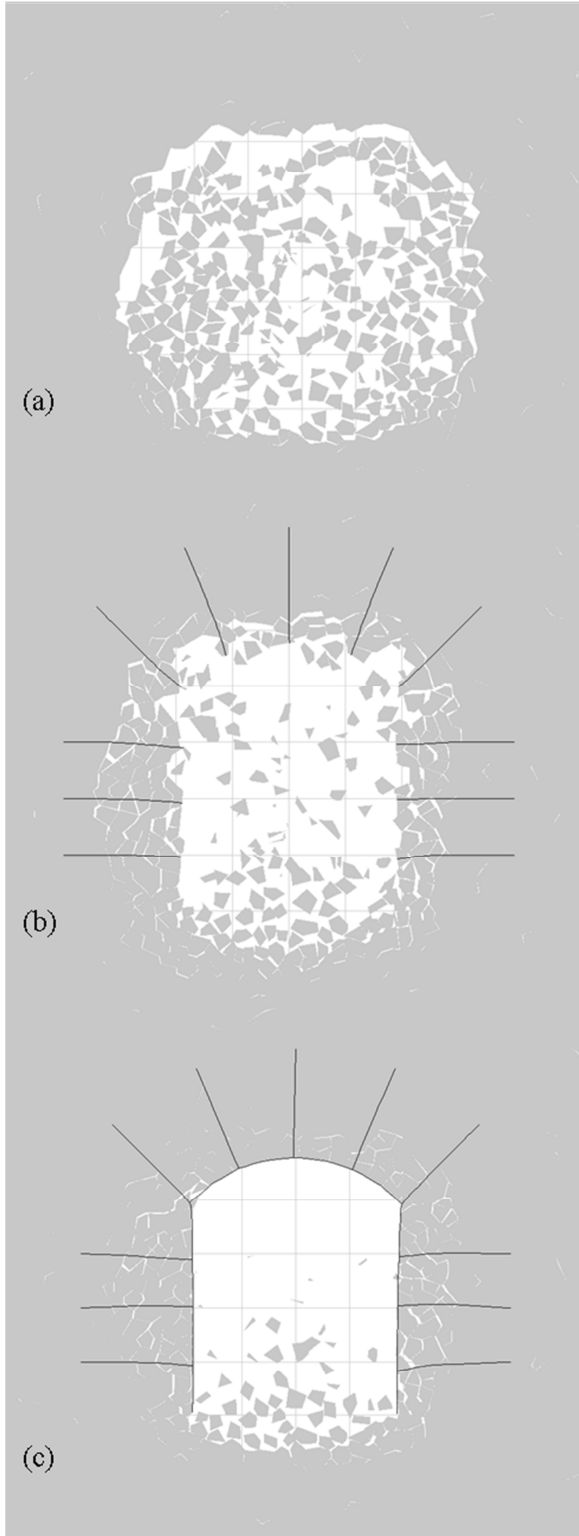


Figure 18: Final model states for (a) unsupported, (b) bolted, (c) bolted and lined excavation subjected to a 60 Hz wave with a PPV of 3.0 m/s and duration of 0.167 sec.

The ground support dissipates the KE of the ejecting rock, maintaining an open passage. It should be mentioned that the increase in KE after the wave has passed (beyond 0.167 sec) is due to gravitational acceleration of the ejected and loosened fragments and would not be considered as part of the energy demand on the ground support system. For the unsupported case, the reduction in KE from 220 kJ to 170 kJ likely occurs because some initially ejected blocks are settling on the floor of the excavation.

The peak values of KE for each of the three cases is similar, as is the fractured area of rock. The ground support has no direct effect on preventing damage to the rock surrounding the excavation; its function is to hold and retain the fractured rock.

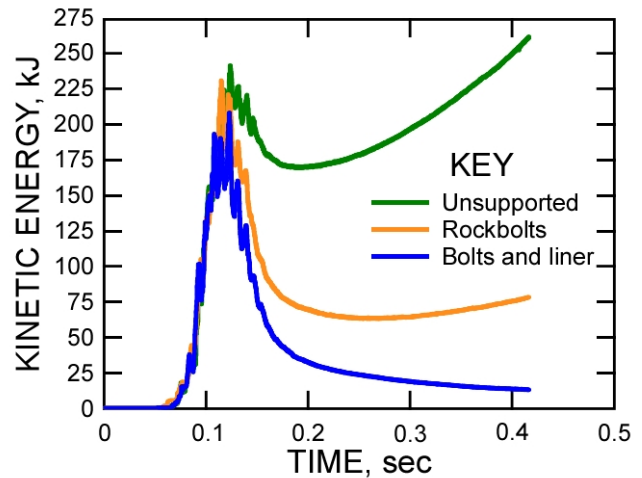


Figure 19: Comparison of kinetic energy of ejecting rock vs. time for unsupported, bolted, and bolted and lined excavations subjected to a 60 Hz wave with a PPV of 3.0 m/s and duration of 0.167 sec.

9. DYNAMIC ENERGY DEMAND

The energy dissipated by the ground support system during dynamic loading was calculated for the 15 equal cycle load cases used in Section 8.1, with the addition of three more combinations of PPV and frequency (2.75 m/s, 40 Hz; 3.5 m/s, 40 Hz; and 2.75 m/s, 60 Hz). Further, KE of ejected rock was calculated for the unsupported cases from Section 6.2. The energy dissipated by the ground support is plotted versus the KE of ejected rock in Figure 20. It is observed that the relationship is well defined by a linear model with a slope of 0.86, indicating that the total energy dissipated by the rockbolts is directly proportional to the KE of the ejecting rock. Additionally, the bolts dissipate a majority of the KE of ejecting rock. The remaining KE is due to

the unsupported rock ejecting from the floor, and rock ejecting between the bolts.

In Figures 21 and 22, energy dissipated by the ground support is plotted versus PPV and PPA, respectively. For low PPV and/or low frequency waves the KE of ejecting rock and the energy dissipated by the ground support is very small. It is noted that vastly different energy demands are placed on the ground support for dynamic loadings of the same PPV but different frequency. In figure 22, it is seen that this result is partially explained by the PPA but that for the same value of peak acceleration, a greater PPV will result in more demand on the ground support. It is clear that neither PPV, nor PPA, fully explains the energy demands on the ground support. Further, a clear PPA threshold is no longer observed. The results suggest that both PPV and PPA are important to understanding dynamic load demand, but the mechanism of dynamic rock failure and ejection cannot be fully characterized by either of these parameters individually.

It is also now clear that volume of ejected rock alone is not a good indicator of the intensity of a rockburst. Two remotely triggered rockbursts caused by different seismic events may result in nearly identical displaced volumes of rock, but the velocities of ejection of the fragments may be significantly different, leading to different energy demands on the support systems.

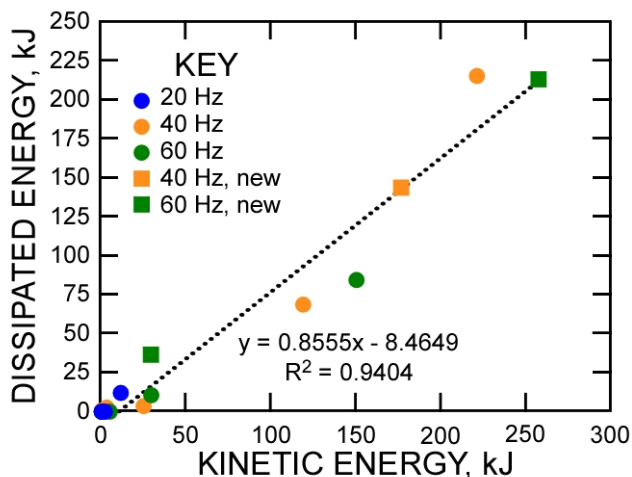


Figure 20: Dissipated energy versus kinetic energy of ejected rock with best-fit linear regression line for waves of equal cycle count.

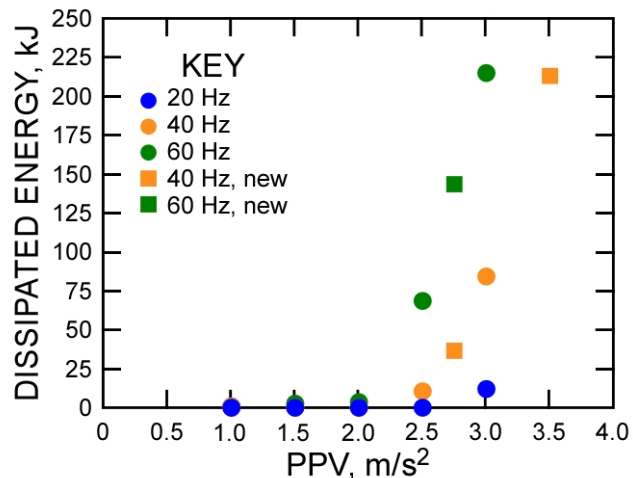


Figure 21: Dissipated energy versus PPV for waves of equal cycle count.

In an attempt to obtain a well-defined relationship between seismic parameters and ground support energy demand, the energy demand on the rockbolts was plotted versus the peak value of the product of velocity and acceleration. The physical significance of this relationship is that the product of velocity and acceleration directly corresponds to power, energy consumed per unit time.

$$P = \frac{E}{t} = \frac{Fd}{t} = Fv = mav \quad (2)$$

where,

- P = power
- E = energy
- t = time
- F = force
- d = distance
- m = mass
- a = acceleration
- v = time

If this quantity is normalized by mass it is called specific power and has units of W/kg. A bi-linear regression model was fit to the data following the form:

$$y = \begin{cases} 0 & , \quad x \leq B \\ A(x - B) & , \quad x > B \end{cases} \quad (3)$$

where A and B are constants, and x and y are the predictor and response variables, respectively. The model results and associated regression are shown in Figure 23. Regression variables are provided in Table 11. Although it is recognized that this trend line has been fit to a relatively limited data set, the regression has an r-square value of 0.98 indicating a near-perfect fit. The use of peak specific power as a predictor variable for this modeled dataset is clearly an improvement compared with the use of PPV or PPA.

The energy demand on the rockbolts can be predicted by the peak specific power associated with the seismic wave. After consideration this is not a surprising result. It suggests that to understand seismic loading, not only is the energy important, but also the rate of application of the energy. More energy isn't necessarily more damaging if it is spread out over a longer duration. Further numerical and empirical investigation is required to better understand dynamic rock damage and support demand. For real waveforms from rockbursts at real mine sites, the problem is undoubtedly more complex, involving not only variable wave parameters but variable mining and geotechnical parameters as well. A multiple parameter approach may often be required to predict dynamic damage or dynamic support demand.

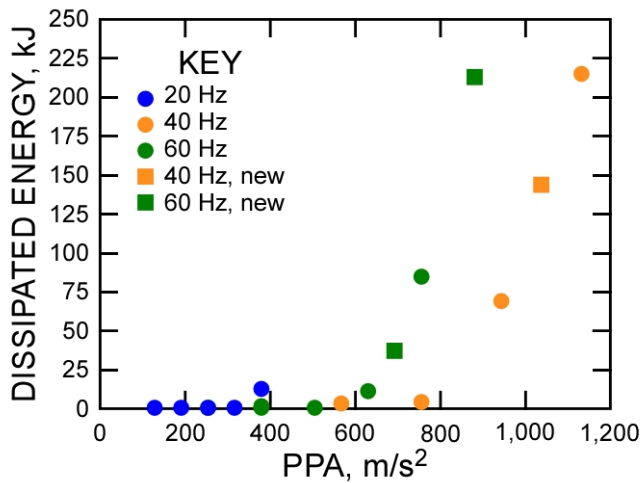


Figure 22: Dissipated energy versus PPAV for waves of equal cycle count.

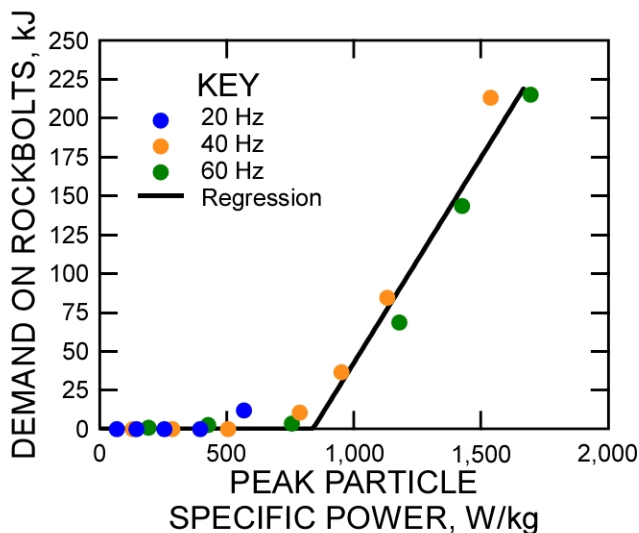


Figure 23: Dissipated energy versus peak particle specific power for waves of equal cycle count.

Table 11. Parameters and goodness of fit for bi-linear regression of rockbolt energy demand versus peak power

Parameter	Value
-----------	-------

A	0.258
B	841.0
SSE	2059
R ²	0.98

10. CONCLUSIONS

The model presented in this paper implies that the dynamic energy demand on ground support is not fully explained by PPA or PPV alone. The demand resulting from seismic events of the same PPV, but different frequency, can vary significantly. This is due to the fact that the accelerations are greater for higher frequency waves. Wave amplitude, duration, and frequency are all important parameters to consider for understanding seismic loading. However, with all other wave and site properties held constant, PPV will be a good indicator of the demand on the support. At mines where PPV correlates well with rockburst damage, it is likely that site parameters, source mechanism and associated wave characteristics do not differ significantly between events of similar magnitude.

The model shows that the product of velocity and acceleration, which is proportional to the peak specific power of the seismic wave, correlates much better with seismic energy demand than either PPV or PPA alone for the dataset presented here. However, this finding should be viewed in full consideration of the limited complexity and range of parameters used in this study. The primary objective is to demonstrate the potential of dynamic modeling and encourage further research.

Lastly, the modeling presented here supports the idea that the main function of ground support (when the loading mechanism is dynamic ejection of rock) is to dissipate the KE of rock ejecting from around the excavation. In the model, the energy that is dissipated by the ground support is linearly proportional to the KE of the ejecting rock in the unsupported case. The rock reinforcement is the main energy dissipating element of the ground support system, but a connected surface support is required to hold the rock mass together and dissipate the energy associated with rock ejecting between reinforcing elements. A complete ground support system including yielding rockbolts and surface support (such as chain-link mesh), as described by Ortlepp (1983), Kaiser et al. (1996), Potvin, and Wesseloo (2010) and others, is required. This is not new, but the model helps understand some principles.

Rockburst loading must be understood in terms of energy. This observation may partially explain why attempts to relate PPV to observed damage are sometimes unsuccessful. Empirical studies should not only record the volume of ejected rock but also the

ejection distance in order to estimate the KE of the rock at time of ejection (via back calculation).

The work presented here is an initial, albeit limited, step due to the complexity of real mine seismicity and rockbursting. Comparison with empirical work is needed to determine the practical value of these insights, and test whether the simple model presented here includes all necessary elements.

Modeling research is required to develop the capability to build models with enough sophistication and complexity to more accurately model dynamic source mechanisms, wave propagation, rock damage and fracture, and ground support. Yet, it is important that incorporation of additional complexity should take place incrementally as not to create confusion. Complexity beyond that which is required to answer a particular question or explain a particular phenomenon is unwarranted. That being said, improvements to, and innovative applications of, modeling software would be very valuable to understanding the science behind complex and currently poorly understood issues in mining seismicity, rockbursting and dynamic support, thus leading to improvements in miner safety and reductions in operational risk.

ACKNOWLEDGEMENT

The authors thank Mark Christianson of Itasca Consulting Group, Inc. for assistance with using SELs in UDEC, developing the energy calculations used in this work, and implementing these calculations into UDEC.

DISCLAIMER

The findings and conclusions in this paper have not been formally disseminated by the National Institute for Occupational Safety and Health and should not be construed to represent any agency determination or policy.

Mention of any company or product does not constitute endorsement by the National Institute for Occupational Safety and Health.

REFERENCES

- Barbour, S.L. and J. Krahn. 2004. Numerical Modeling Prediction or Process? *Geotechnical News*, 44–52.
- Barton, N., and H. Hansteen. 1979. Very large span openings at shallow depth: deformation magnitudes from jointed models and finite element analysis. Paper presented at the *4th Rapid Excavation and Tunneling Conference*, Atlanta, GA.
- Bauer, A., and P.N. Calder. 1970. The Influence and Evaluation of Blasting on Stability. Paper presented at the *1st International Conference on Stability in Open Pit Mining*, Vancouver, BC.
- Biggs, J.M. 1964. *Introduction to Structural Dynamics*. McGraw Hill. New York, NY.
- Brady, B.H. 1990. *Dynamic performance and design of underground excavations in jointed rock*. Rotterdam: Balkema.
- Christianson, M. 2015. Energy Calculation Modifications in UDEC 6.0. 2-1607-01. Prepared by Itasca Consulting Group, Minneapolis, MN, for NIOSH Spokane Research Center, Spokane, WA.
- Cichowicz, A., A.M. Milev and R.J. Durrheim. 2000. Rock mass behaviour under seismic loading in a deep mine environment: implications for stope support. *The Journal of South African Institute of Mining and Metallurgy* 100(2): 121–128.
- Dowding, C.H. 1985. *Blast Vibration Monitoring and Control*: Library of Congress.
- Dowding, C.H., and A. Rozen. 1978. Damage to rock tunnels from earthquake shaking. *Journal of Geotechnical Engineering Division American Society of Civil Engineers*, 104, 175–191.
- Dowding, C.H., C. Ho and T.B. Belytschko. 1983. Earthquake Response of Caverns in Jointed Rock: Effects of Frequency and Jointing. Proceedings of *Seismic Design of Embankments and Caverns*. American Society of Civil Engineers. Philadelphia, PA, May 16-20, pp. 142–156.
- Durrheim, R.J., M.K.C. Roberts, A.T. Haile, T.O. Hagan, A.J. Jager, M.F. Handley, S.M. Spottiswoode and W.D. Ortlepp. 1998. Factors influencing the severity of rockburst damage in South African gold mines. *The Journal of South African Institute of Mining and Metallurgy* 98(2): 53–57.
- Hendron, A.J. 1977. *Engineering of Rock Blasting on Civil Projects*. Englewood Cliffs, NJ: Prentice Hall.
- Hsiung, S.M., A.H. Chowdhury, W. Blake, M.P. Ahola and A. Ghosh. 1992. Field Site Investigation: Effect of Mine Seismicity on a Jointed Rock Mass. CNRWA 92-012: Center for Nuclear Waste Regulatory Analysis, San Antonio, TX.
- Hsiung, S.M. and A. Ghosh. 2006. Seismic Responses of Underground Excavations in Jointed Rock Mass. Paper presented at the *41st U.S. Symposium on Rock Mechanics*, Golden, CO.
- Hammah, R.E. and J.H. Curran. 2009. It is better to be Approximately Right than Precisely Wrong – Why Simple Models Work in Mining Geomechanics. Paper presented at the *43rd US Rock Mechanics Symposium*, Asheville, NC, 2009.
- Itasca Inc. 2015. Universal Distinct Element Code (UDEC v6.0) User Manual. Itasca Consulting Group, MN.
- Kaiser P.K., D.D. Tannant and D.R. McCreath. 1996. *Canadian rockburst support handbook*. Sudbury, Ontario: Geomechanics Research Centre, Laurentian University, 1996.

- Kuhlemeyer, R.L., and J. Lysmer. 1973. Finite Element Method Accuracy for Wave Propagation Problems. *Journal of Soil Mechanics and Foundations Division of the American Society for Civil Engineers*, 99(SM5), 421–427.
- Labreche, D.A. 1983. Damage Mechanisms in Tunnels Subjected to Explosive Loads. Proceedings of *Seismic Design of Embankments and Caverns*. American Society of Civil Engineers. Philadelphia, PA, May 16-20, 1983, 128–140.
- Langefors, U. and B. Kihlstrom. 1963. *The Modern Technique of Rock Blasting*. New York, NY: John Wiley and Sons.
- Ma, M. and B.H. Brady. 1999. Analysis of the Dynamic Performance of an Underground Excavation in Jointed Rock under Repeated Seismic Loading. *Geotechnical and Geological Engineering*, 17(1), 1–20.
- McGarr, A., R.W.E. Green and S.M. Spottiswoode. 1981. Strong Ground Motion of Mine Tremors: Some implications for near-source ground motion parameters. *Bulletin of the Seismological Society of America*, 71, 295–319.
- McGarr, A. 1983. Estimating Ground Motions for Small nearby Earthquakes. Proceedings of *Seismic Design of Embankments and Caverns*. American Society of Civil Engineers. Philadelphia, PA, May 16-20, 1983, 113–126.
- Ortlepp, W.D. 1983. Considerations in the design of support for deep hard-rock tunnels. Proceedings of the *5th International Congress of the International Society for Rock Mechanics*, Melbourne, Australia, pp. D179–187.
- Player, J.R., E.C. Morton and E. Villaescusa. 2008. Static and dynamic testing of steel wire mesh for mining applications of rock surface support. Proceedings of the *6th International Symposium on Ground Support in Mining and Civil Engineering Construction*, Cape Town, Republic of South Africa, pp. 693–706.
- Potvin, Y., J. Wesseloo and D. Heal. 2010. An interpretation of ground support capacity submitted to dynamic loading. Proceedings of the *5th International Seminar on Deep and High Stress Mining*, Santiago, Chile, pp. 251–272.
- Raffaldi, M.J. and M.C. Loken. 2016. Rock Mass modeling approach for simulating wave propagation, rock fracture, and rock ejection. Paper presented at the *50th US Rock Mechanics Symposium*, Phoenix, AZ, 2016 (this conference).
- Sharma, S. and W.R. Judd. 1991. Underground opening damage from earthquakes. *Engineering Geology*, 30, 263–276.
- Stacey, T.R. 2012. A Philosophical view on the testing of rock support for rockburst conditions. *The Journal of South African Institute of Mining and Metallurgy*, Volume 112: 97–104.
- Starfield, A.M. and P.A. Cundall. 1988. Towards a methodology for rock mechanics modelling. *International Journal of Rock Mechanics and Mining Science*, 24(3): 99–106
- St John, C.M., and T.F. Zahrah. 1987. Aseismic design of underground structures. *Tunnelling and Underground Space Technology*, 2(2), 165–197.
- Wagner, H. 1984. Support requirements for rockburst conditions. Proceedings of the *1st International Congress on Rockburst and Seismicity in Mines*, Johannesburg, Republic of South Africa, pp. 209–218.